Bone as a microcontinuum[1] [2]

Josef Rosenberg & **Robert Cimrman** & **Luděk Hynčík**

University of West Bohemia in Plzeň
Department of Mechanics & New Technology Research Centre
Univerzitní 22, 301 14 Plzeň

How to treat the microstructure?

- homogenization
- theory of mixtures, of composites
- microcontinuum theories

[1] Presentation for the conference **Výpočtová Mechanika 2001**, Nečtiny, 29.-31. October 2001.
[2] Typeset by ConTEXt (`http://www.pragma-ade.nl`).

Basic kinematics

- Continuum "points" can translate, but also rotate and deform
  $\longrightarrow$ micromorphic continuum.
- Position within a particle given by $\underline{x}' = \underline{x} + \underline{\xi}$, $\underline{y}' = \underline{y} + \underline{\eta}$.
- Special types:
  - microstretch continuum: rotation + volume change,
  - micropolar continuum: rotation only.

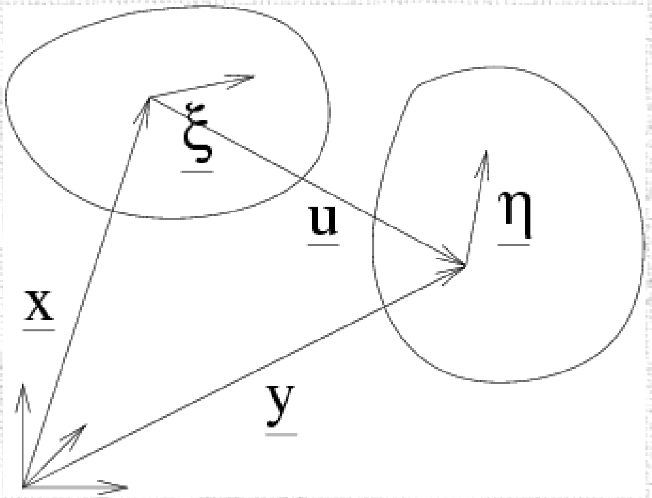

Figure 1 Coordinates within particles.

General balance equations

The balance of forces and balance of stress moments equations:

$$t^{kl}{}_{,k} + \rho f^l = 0 \,, \qquad m^{klm}{}_{,k} + t^{ml} - s^{ml} + \rho l^{lm} = 0 \,. \tag{1}$$

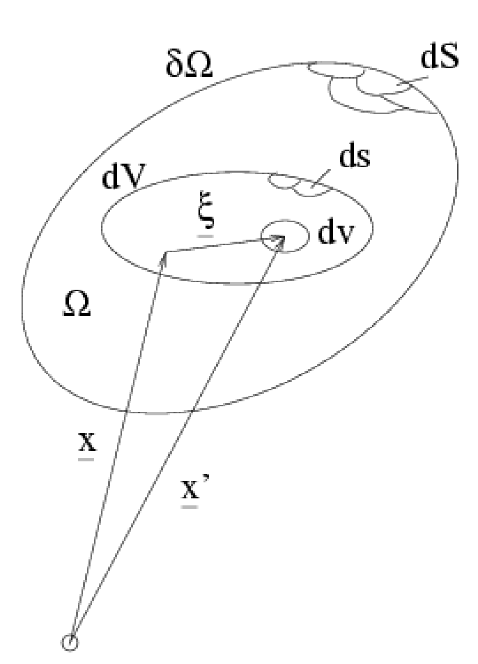

t'^{kl}	...	stress tensor in a particle, $t'^{kl} = t'^{lk}$,
s^{lm}	...	micro-stress average — stress tensor of the macrovolume averaged across the volume (symmetric),
t^{kl}	...	stress tensor of the macrovolume averaged across the surface (non-symmetric),
m^{klm}	...	the first stress moment — moment of the forces acting on the surface of the macrovolume with respect to its centre of gravity,
l^{lm}	...	the first body moment of the volume forces with respect to the centre of gravity of the macrovolume,
f^l	...	averaged volume force.

Some defining relations: $\int\limits_{\mathrm{d}S} t'^{kl} n'_k \,\mathrm{d}s' = t^{kl} n_k \,\mathrm{d}S \,, \quad \int\limits_{\mathrm{d}S} \xi'^m t'^{kl} n'_k \,\mathrm{d}s' = m^{klm} n_k \,\mathrm{d}S \,.$

Special types

- **microstretch continuum** — 7 degrees of freedom

$$m^{klm} = \frac{1}{3} m^k \delta^{lm} - \frac{1}{2} e^{lmr} m^k{}_r \,, \tag{2}$$

$$l^{kl} = \frac{1}{3} l \delta^{lm} - \frac{1}{2} e^{klr} l_r \,. \tag{3}$$

- **micropolar continuum** — 6 degrees of freedom

$$m^k = 0 \,, \quad l = 0 \,. \tag{4}$$

Micropolar continuum - the boundary value problem

- Basic equations:

$$t^{kl}{}_{,k} + \rho f^l = 0 \, , \qquad m^k{}_{l,k} + e_{lmn} t^{mn} + \rho l_l = 0 \, , \tag{5}$$

$$t_{kl} = \rho \frac{\partial \Psi}{\partial \overline{\Psi}_{KL}} \frac{\partial y_k}{\partial x^K} \overline{\chi}_{lL} \, , \quad m_{kl} = \rho_0 \frac{\partial \Psi}{\partial \Gamma_{LK}} \frac{\partial y_k}{\partial x^K} \overline{\chi}_{lL} \, ,$$

$$\overline{\Psi}_{KL} = y^k_{,K} \, \overline{\chi}_{kL} \, , \quad \Gamma_{KL} = \frac{1}{2} e_K{}^{MN} \overline{\chi}_{kM} \overline{\chi}_{kN} \, , \text{ where } \chi^l_k = \frac{\partial \eta^l}{\partial \xi^k} \, , \, \overline{\chi}^l_k = \frac{\partial \xi^l}{\partial \eta^k} .$$

- For the isotropic continuum holds (denoting $\gamma_{ij} = \phi_{i,j}$, $\varepsilon^{kl} = \frac{\partial u^l}{\partial x^k} + e^{lkm} \phi_m$):

$$t_{kl} = \lambda \varepsilon^m_m \delta_{kl} + (\mu + \kappa) \varepsilon_{kl} + \mu \varepsilon_{lk} \, , \qquad m_{kl} = \alpha \gamma^m_m \delta_{kl} + \beta \gamma_{kl} + \gamma \gamma_{lk} \, . \tag{6}$$

- The boundary conditions: $\left. \begin{array}{c} u_k = \hat{u}_k \\ \phi_k = \hat{\phi}_k \end{array} \right\}$ on $\partial \Omega_1$, $\left. \begin{array}{c} t_{kl} n^k = \hat{t}_l \\ m_{kl} n^k = \hat{m}_l \end{array} \right\}$ on $\partial \Omega_2$.

Variational formulation

The solution is the stationary point of the potential (see **[8]**)

$$
\begin{aligned}
\Pi(\underline{u}, \underline{\phi}) \; &= \tfrac{1}{2} \int_\Omega \left[\lambda \delta^{kl} \varepsilon_m^m + (\mu + \kappa)\varepsilon^{kl} + \mu \varepsilon^{kl}\right] \varepsilon_{kl} \mathrm{d}x \\
&+ \tfrac{1}{2} \int_\Omega \left(\alpha \delta^{kl} \gamma_m^m + \beta \gamma^{kl} + \gamma \gamma^{lk}\right) \gamma_{lk} \mathrm{d}x + \int_{\partial\Omega_2} (\hat{u}_i n_j + g_{ij}) \tau^{ij} \mathrm{d}x \\
&+ \int_{\partial\Omega_2} (\hat{\phi}_k n_l + \gamma_{kl}) m^{kl} \mathrm{d}x - \int_\Omega \rho \hat{f}_i u_i \mathrm{d}x - \int_{\partial\Omega_1} \hat{\tau}_i u_i \mathrm{d}x - \int_\Omega \rho \hat{l}^l \phi_l \mathrm{d}x
\end{aligned}
$$

with the constraints

$$
\varepsilon^{kl} = \frac{\partial u^l}{\partial x^k} + e^{lkm}\phi_m, \quad -u_i n_j = g_{ij} \text{ on } \partial\Omega_2, \quad \gamma^{kl} = \frac{\partial \phi_k}{\partial x^l}, \quad -\phi_i u^j = \gamma^{ij} \text{ on } \partial\Omega_2\,.
$$

The weak solution of the problem at **page 5** satisfies (we omit loading terms here)

$$
\Pi(\underline{u}, \underline{\phi}; \delta\underline{u}) = 0 \rightarrow \int_\Omega \tau_{kl} \delta_u \varepsilon_{kl} \mathrm{d}\Omega = 0, \tag{7}
$$

$$
\Pi(\underline{u}, \underline{\phi}; \delta\underline{\phi}) = 0 \rightarrow \int_\Omega \left(\tau_{kl} \delta_\phi \varepsilon_{kl} + m_{kl} \delta_\phi \phi_{l,k}\right) \mathrm{d}\Omega = 0\,. \tag{8}
$$

FE discretization

Denote: $\mathbf{1} \equiv [1,1,1|0,0,0|0,0,0]^T$, $\mathbf{J}$ . . . a permutation matrix, $\mathbf{G}$, ν strain operators.

$$\mathbf{t}^e = \underbrace{(\lambda \mathbf{1}\mathbf{1}^T + (\mu+\kappa)\mathbf{I} + \mu\mathbf{J})}_{\mathbf{D}_1}[\mathbf{G}^+|\nu]\mathbf{d}^e = \mathbf{D}_1\mathbf{B}\mathbf{d}^e\,,\; \mathbf{m}^e = \underbrace{(\alpha\mathbf{1}\mathbf{1}^T + \beta\mathbf{J} + \gamma\mathbf{I})}_{\mathbf{D}_2}\mathbf{G}^+\phi^e = \mathbf{D}_2\mathbf{G}^+\phi^e\,.$$

Discrete balance equations for one element:

$$U_e \equiv \sum_q \left[\mathbf{G}^{+T}\mathbf{t}^e J_0 W\right]|_{\xi^q} = \sum_q \left[\mathbf{G}^{+T}\mathbf{D}_1\mathbf{B}J_0W\right]|_{\xi^q}\cdot\mathbf{d}^e = [A_e, B_e]\mathbf{d}^e = 0\,, \qquad (\leftarrow \textbf{Eq. 7})$$

$$\begin{aligned}\phi_e \equiv\ & \sum_q \left[(\nu^T\mathbf{t}^e + \mathbf{G}^{+T}\mathbf{m}^e)J_0W\right]|_{\xi^q} = \sum_q\left[\nu^T\mathbf{D}_1\mathbf{B}J_0W\right]|_{\xi^q}\cdot\mathbf{d}^e \\ & + \sum_q\left[\mathbf{G}^{+T}\mathbf{D}_2\mathbf{G}^+J_0W\right]|_{\xi^q}\cdot\phi^e = [C_e, D_e]\mathbf{d}^e + E_e\phi^e = 0\,. \qquad (\leftarrow \textbf{Eq. 8})\end{aligned}$$

$\Rightarrow$ Linear system with indefinite matrix:

$$\begin{bmatrix} A_e & B_e \\ C_e & D_e + E_e \end{bmatrix}\begin{bmatrix}\mathbf{u}^e \\ \phi^e\end{bmatrix} = \begin{bmatrix} f^e \\ g^e\end{bmatrix}\,. \qquad (9)$$

Analytical verification I

The analytical solution is known in some cases (cf. **[3]**, results taken from **[8]**) , e.g.:

- a plane with a hole loaded in tension,
- compute the stress concentration factor on the boundary of the hole.

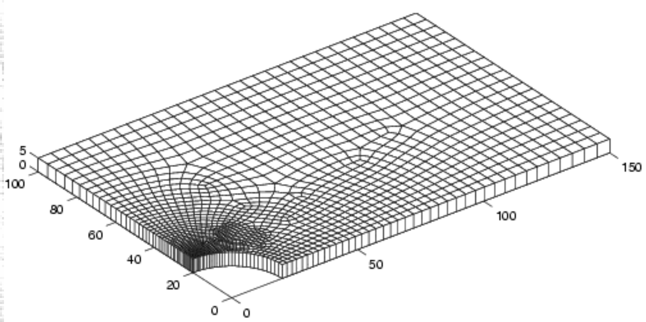

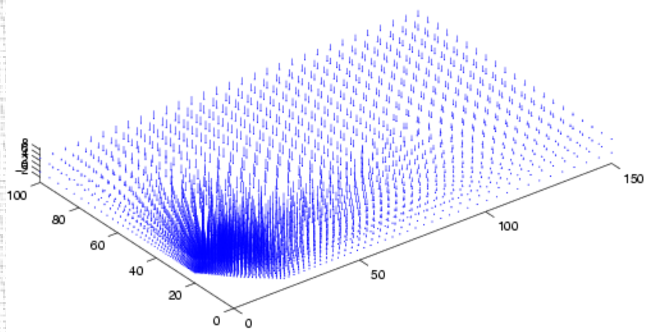

mesh microrotations

Figure 2 Plane with a hole.

Analytical verification II

R = radius of the hole (macroscopic characteristic length) [m]
c = characteristic length of the microstructure [m]
K = stress concentration factor

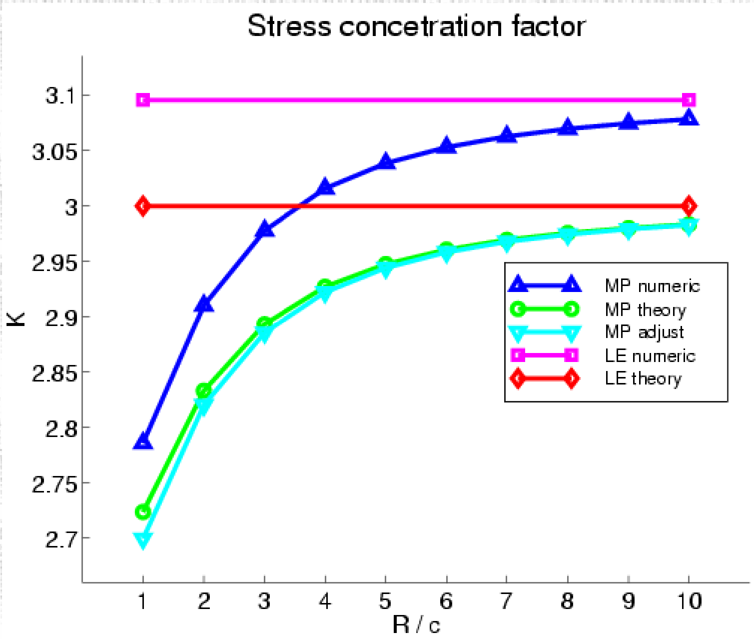

Figure 3 Stress concentration(R/c).

Theory:

- linear elasticity: red curve ($K = 3$)
- micropolar elasticity: green curve

Numerical values:

- linear elasticity: magenta curve
- micropolar elasticity: blue curve
- adjusted (shifted by LE numeric – LE theory): cyan curve

Femur bone with nail — motivation

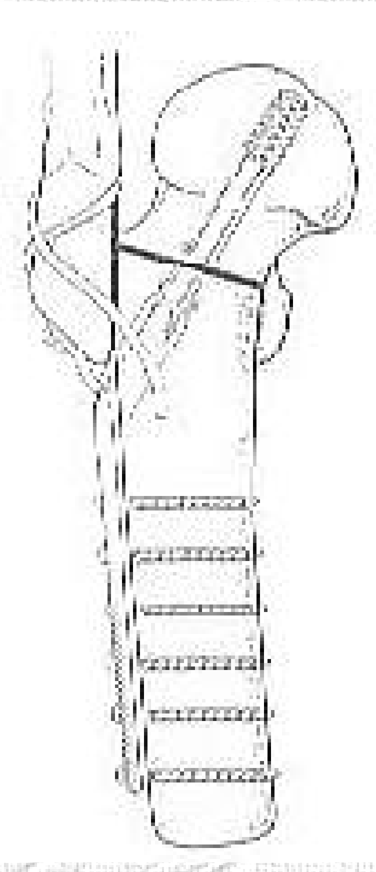

Figure 4 Example of a fixation of a bone.

Femur bone with nail — material data

set	λ [Pa]	μ [Pa]	κ [Pa]	α [N]	β [N]	γ [N]
MP1	$1.8 \cdot 10^{10}$	$-1.468 \cdot 10^{10}$	$3.837 \cdot 10^{10}$	-120	120	240
MP2	$1.8 \cdot 10^{10}$	$-1.468 \cdot 10^{10}$	$3.837 \cdot 10^{10}$	-12000	12000	24000
LE	$1.8 \cdot 10^{10}$	$4.5 \cdot 10^{9}$	—	—	—	—

Table 1 Material data.

- Equivalent LE set was obtained using $\lambda_E = \lambda_M$, $\mu_E = \mu_M + \kappa/2$ ($\rightarrow E = 1.26 \cdot 10^{10}$ [Pa], $\nu = 0.4$).
- Material data of the steel nail: $E = 2.1 \cdot 10^{11}$ [Pa], $\nu = 0.3$.
- Characteristic lengths of the microstructure:
  - MP1: $c = 0.1283$ [mm]
  - MP2: $c = 1.283$ [mm]
- Characteristic length of the macrostructure = radius of the hole.
- LE set was used in PAM-Crash code for verification of our solver — the results are denoted as "PC".

Femur bone with nail — loads

- Two kinds of loading: bending and torsion.
- Observed micropolar effect: decrease of stress on the femur–nail interface

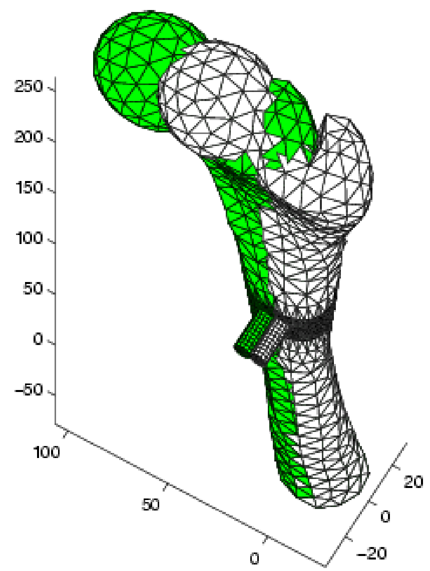

bending

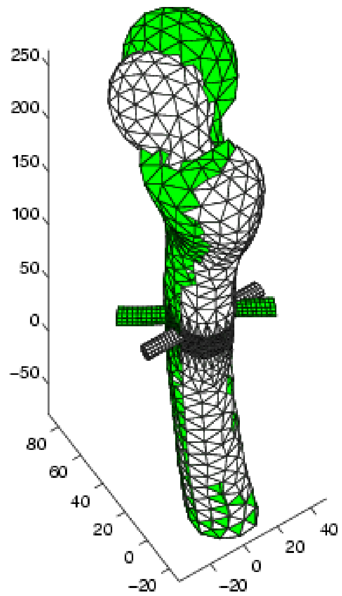

torsion

Figure 5 Original (white) + deformed femur mesh (magnified displacements), LE set used for the bone.

Femur bone with nail — evaluation lines

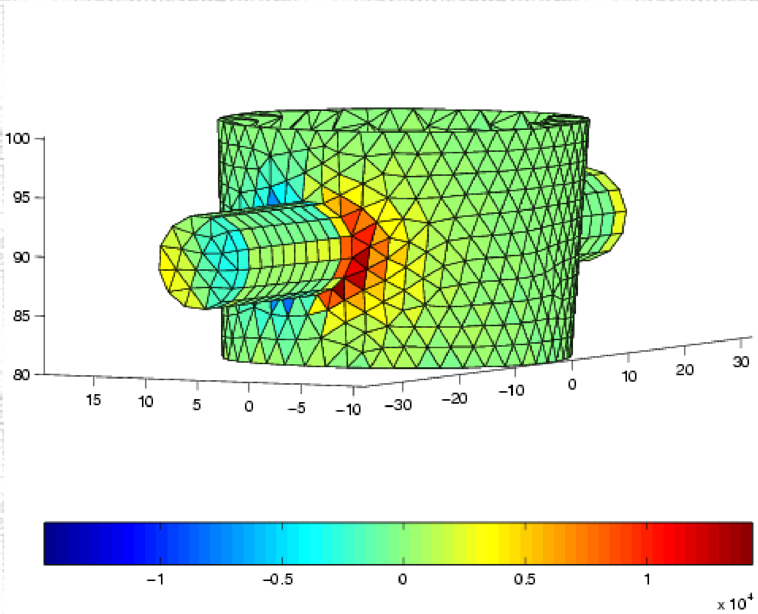

Figure 6 t_{22} [kPa], torsion case.

The nail was considered to be fixed to the bone — no movement between the two materials was allowed. The stress was evaluated along these lines on the surface of the hole drilled into the bone:

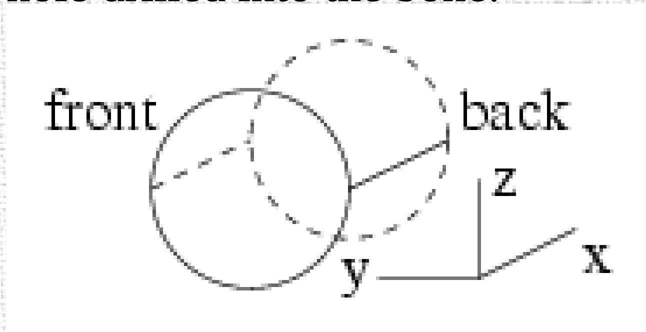

Femur bone with nail — stress along the lines

- Bending load: different behaviour (tension-compression) of middle and "non-middle" rows of elements $\Rightarrow$ separate plots.
- Torsion load: no such phenomenon.

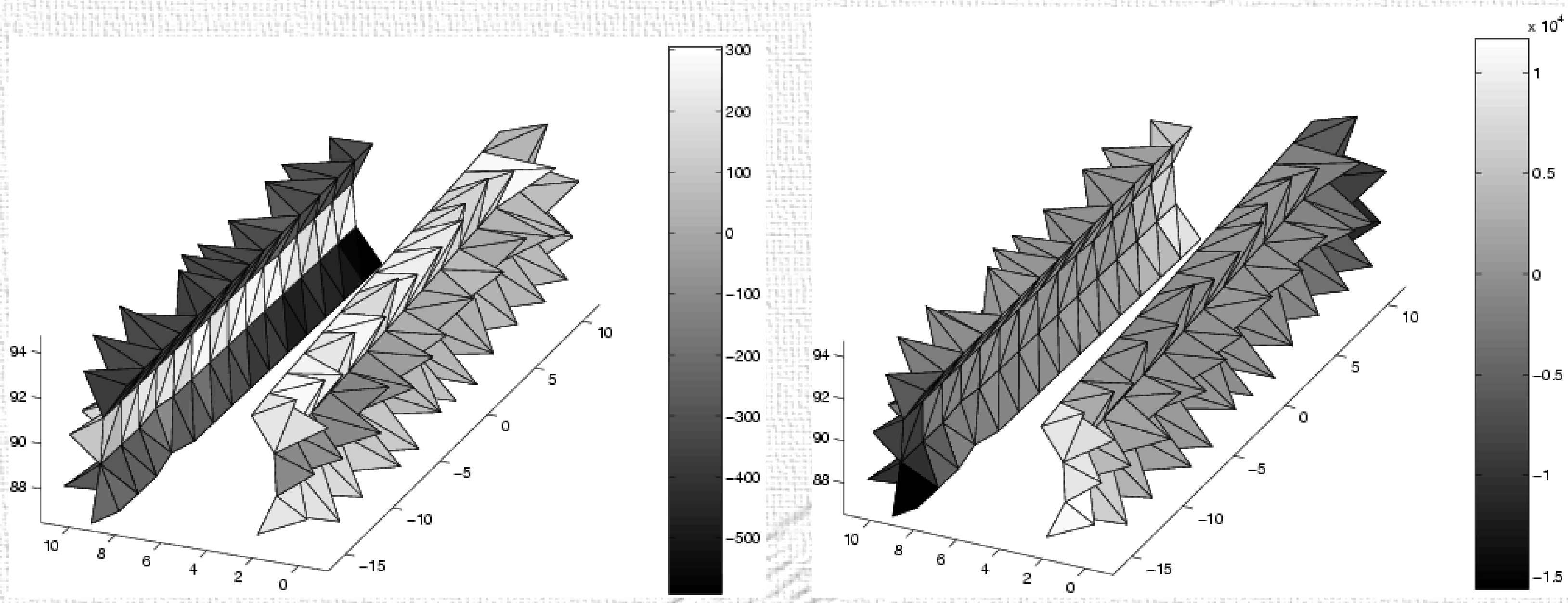

t_{33} [kPa] (bending) t_{22} [kPa] (torsion)

Figure 7 Stress along the lines, MP2 set used for the bone.

Femur bone with nail — example Ia

- We plot "averaged" stress along the front and back lines of Figure at **page 13**.
- The "averaging" = the least squares fitting of stress in the elements of **Figure 7**).

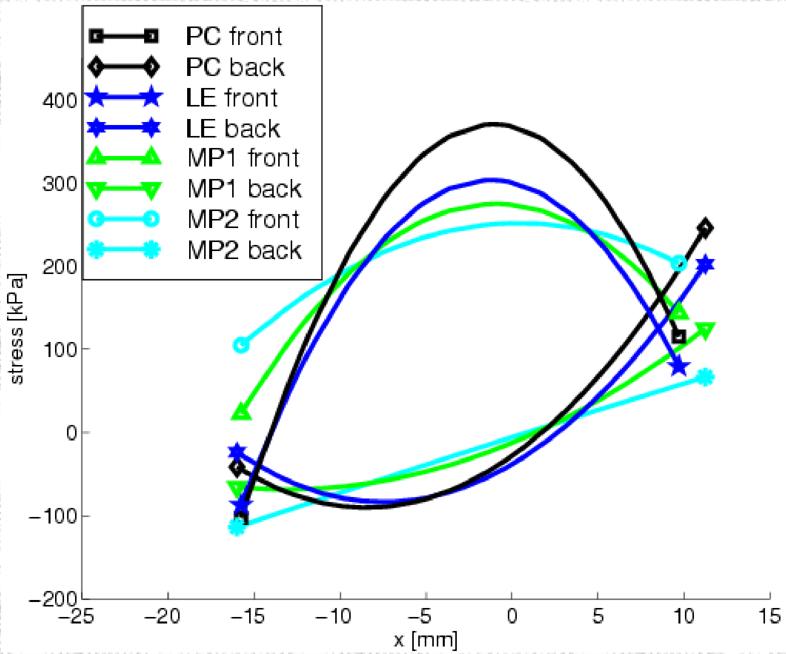

middle element row

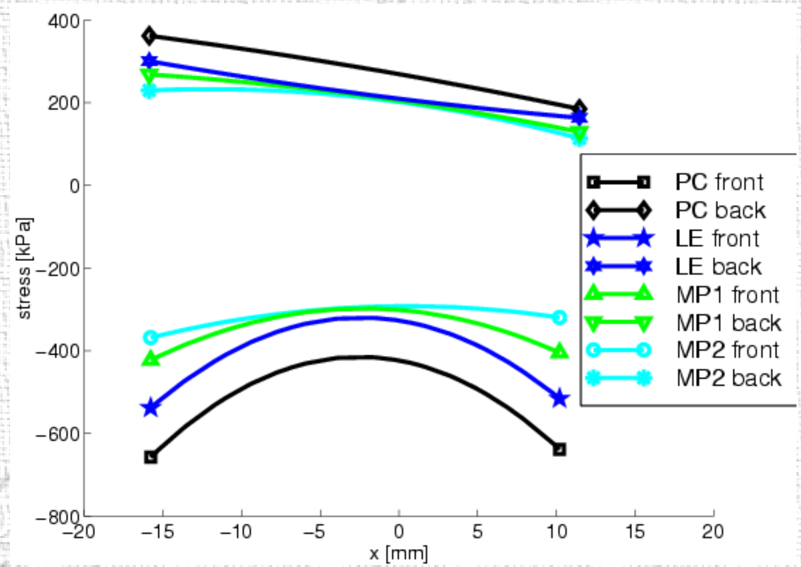

upper element row

Figure 8 t_{33} along the lines, bending.

Femur bone with nail — example Ib

- The bending case — fitting with the second order polynomial.
- The torsion case — fitting with the third order polynomial.

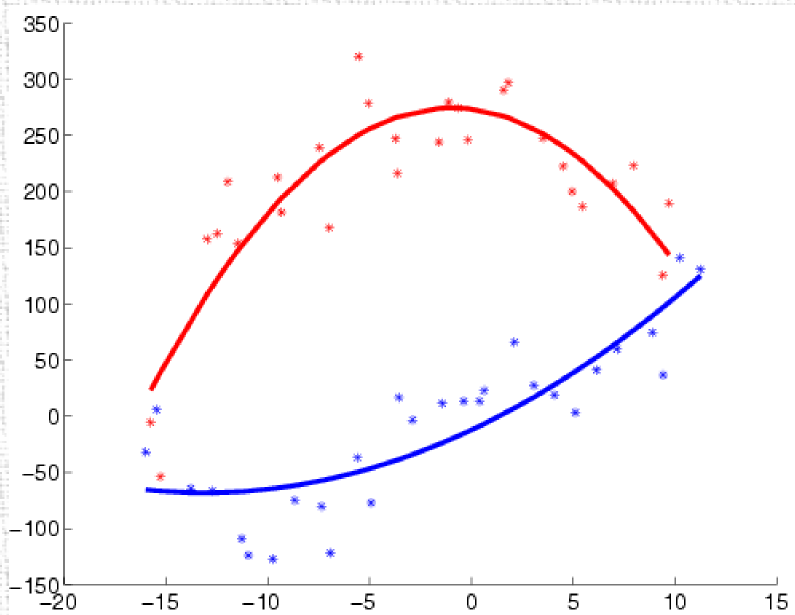

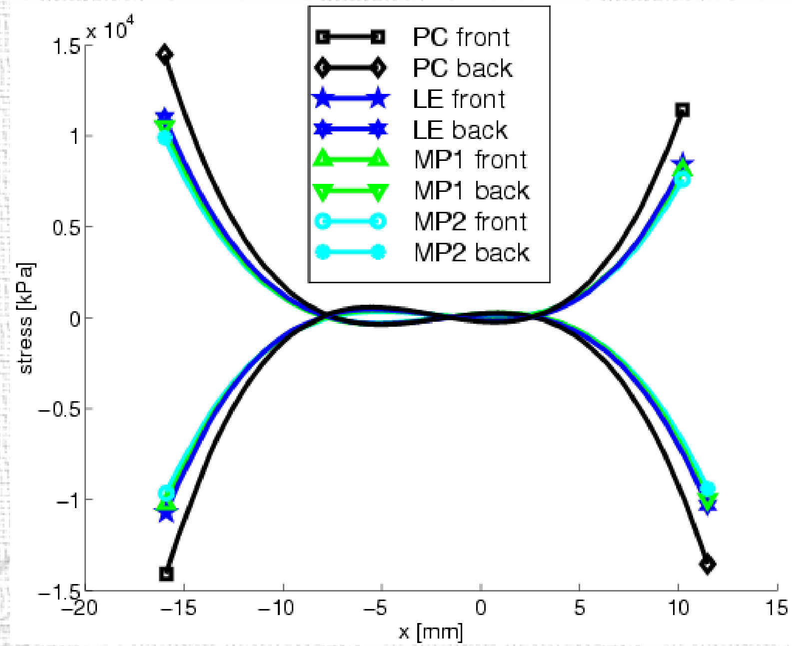

Bending, middle element row, MP1 set. t_{22} along the lines, torsion.

Figure 9 Averaging example + torsion case results.

Femur bone with nail — example IIa

- Dependence of stress on c: l_t varied in range $\langle 0.2, 2\rangle$ [mm] while keeping the other parameters constant. This resulted in c variation in range $\langle 0.1283, 1.283\rangle$ [mm].
- Stress was evaluated in 6 selected elements (“left” end of the hole (the lowest x coordinate), see **Figure 7**, **Table 2**.
- Note the difference between middle and non-middle elements in the bending case.

element	5786	4236	4351	6103	6050	6123
line	front	front	front	back	back	back
row	upper	middle	lower	upper	middle	lower

Table 2 Selected elements.

Femur bone with nail — example IIb

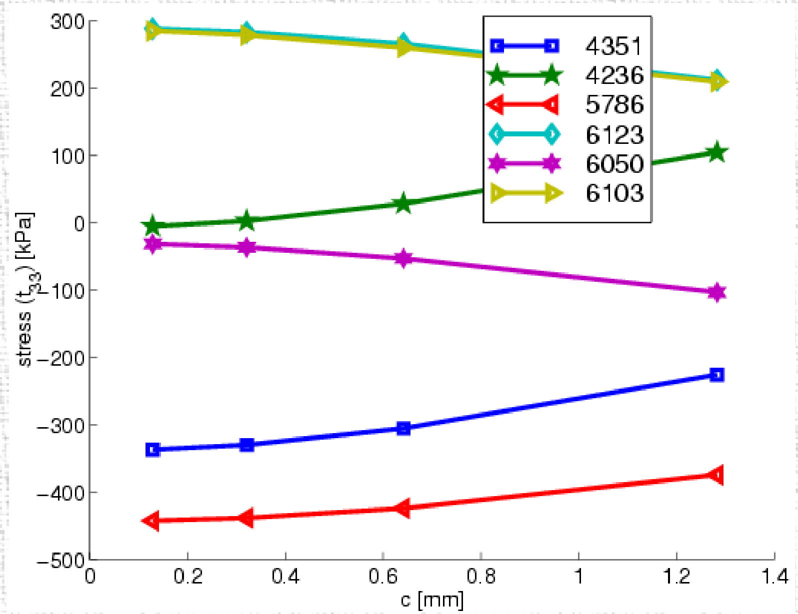

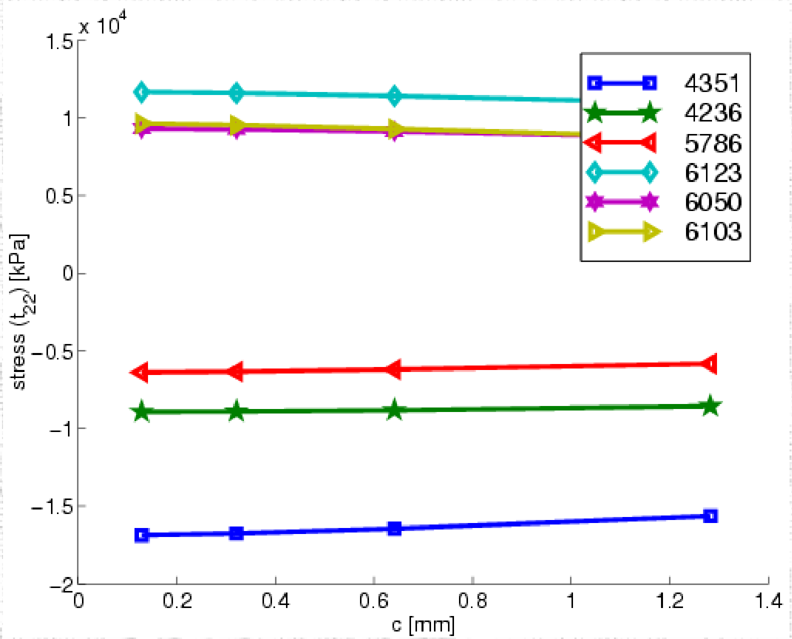

$t_{33}(c)$, bending $\qquad$ $t_{22}(c)$, torsion

Figure 10 Dependence on c in the selected elements.

Femur bone with nail — example IIc

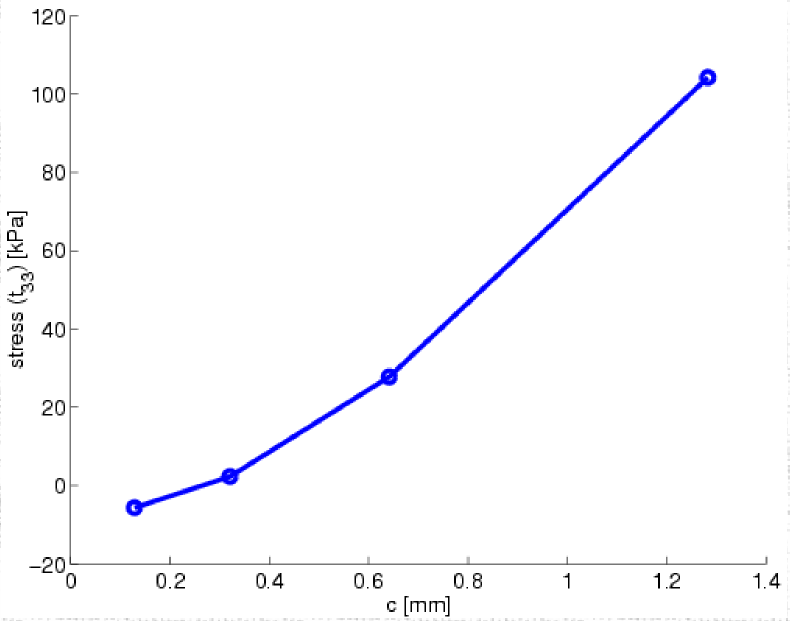

$t_{33}(c)$, bending

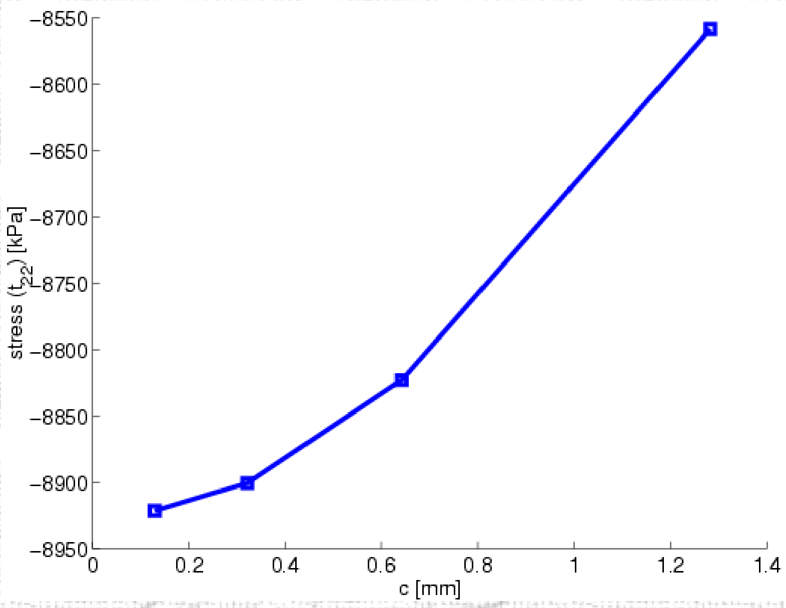

$t_{22}(c)$, torsion

Figure 11 Dependence on c in element 4236.

Conclusion

- Linear micropolar elasticity was introduced.
- Presented examples showed a strong influence of the microstructural parameters on the stress.
- Further work:
  - micropolar anisotropic continuum
  - micromorphic continuum
  - material parameter identification

References

[1] H. Bufler. Zur variationsformulierung nichtlinearer randwertprobleme. *Ingenieur-Archiv 45*, pp. 17–39, 1976.

[2] E. Cosserat. *Theorie des Corps Deformables*. Hermann, Paris, 1909.

[3] A.C. Eringen. *Microcontinuum Field Theories: Foundation and Solids*. Springer, New York, 1998.

[4] A.C. Eringen and E.S. Suhubi. Nonlinear theory of simple micro-elastic solids. *Int. J. Engng. Sci.*, 2:189–203, 1964.

[5] H.C. Park and R.S. Lakes. Cosserat micromechanics of human bone: Strain redistribution by a hydratation sensitive constituent. *J. Biomechanics*, 19:385–397, 1986.

[6] J. Rosenberg. Allgemeine variationsprinzipien in den evolutionsaufgaben der kontinuumsmechanik. *ZAMM*, 65:417–426, 1985.

[7] J. Rosenberg. Variational formulation of the problems of mechanics and its matrix analogy. *Journal of Computational and Applied Mathematics*, 53:307–311, 1995.

[8] J. Rosenberg and R. Cimrman. Microcontinuum Approach in Biomechanical Modelling. *Mathematics and Computers in Simulation*, 2001. Special volume: Proceedings of the conference Modelling 2001, Plzeň, submitted.